VSIG4 overexpression alleviates acute kidney injury of mice via inhibition of M1-macrophages activation

Yan Li, Yong Liu, Furong Li, Yiqin Wang, Kailong Wang, Jinghong Zhao

Department of Nephrology, Xinqiao Hospital, Army Medical University (Third Military Medical University), Chongqing, China

Contributions: (I) Conception and design: J Zhao, Y Li; (II) Administrative support: J Zhao; (III) Provision of study materials or patients: Y Li, F Li; (IV) Collection and assembly of data: Y Li, Y Wang, K Wang; (V) Data analysis and interpretation: J Zhao, Y Li; (VI) Manuscript writing: All authors; (VII) Final approval of manuscript: All authors.

Correspondence to: Jinghong Zhao. Department of Nephrology, the Key Laboratory for the Prevention and Treatment of Chronic Kidney Disease of Chongqing, Chongqing Clinical Research Center of Kidney and Urology Diseases, Xinqiao Hospital, Army Medical University (Third Military Medical University), 83 Xinqiao Street, Shapingba District, Chongqing 400037, China. Email: zhaojh@tmmu.edu.cn.

Background: The infiltration and activation of M1-macrophages can promote renal tubular interstitial damage. The study aimed to investigate the effect of V-set and immunoglobulin domain containing 4 (VSIG4) on M1-macrophages activation and acute kidney injury (AKI) mice.

Methods: The M1-macrophage markers cluster of differentiation 86 (CD86) and inducible nitric oxide synthase (iNOS) were detected via flow cytometry. Cell viability and expression of inflammatory factors were analyzed through 3-(4,5-dimethylthiazol-2-yl)-2,5-diphenyl tetrazolium bromide (MTT), 5-ethynyl-2'-deoxyuridine (EdU), as well as quantitative polymerase chain reaction (qPCR) and enzyme-linked immunosorbent assay (ELISA) assays. Moreover, HK-2 cells stimulated with lipopolysaccharide (LPS) and RAW264.7 cells overexpressing VSIG4 were co-cultured to analyze the effect of VSIG4 suppressing M1-macrophage activation on HK-2 cells via detecting cell proliferation and apoptosis levels. Furthermore, the pathological changes and iNOS expression of kidney tissue in VSIG4 knockout mice with renal ischemia-reperfusion injury (IRI) were detected by hematoxylin and eosin (H&E) and immunohistochemistry (IHC) staining.

Results: Overexpression of VSIG4 partially reversed the phenomenon of M1-macrophageactivation caused by LPS-upregulated CD86 and iNOS expression, reduced cell viability, and induced the expression levels of interleukin 1β (IL-1β), interleukin 6 (IL-6), and tumor necrosis factor-α (TNF-α) in RAW264.7. In addition, RAW264.7 cells overexpressing VSIG4 could also alleviate the low proliferation and high apoptotic level of HK-2 cells stimulated with LPS. After VSIG4 knockout, the kidney tissue of AKI mice showed obvious lesions and iNOS expression, indicating that VSIG4 knockout promoted the infiltration of M1-macrophages in the damaged kidney tissue and accelerated kidney tissue lesions.

Conclusions: Overexpression of VSIG4 might alleviate the lesions of kidney tissue in AKI mice via inhibition of the secretion of inflammatory factors in M1-macrophages.

Keywords: V-set and immunoglobulin domain containing 4 (VSIG4); M1-macrophages; acute kidney injury (AKI); apoptosis; HK-2 cells

Page 2 of 14

Li et al. VSIG4 overexpression inhibits M1-macrophages activation

Introduction

Acute kidney injury (AKI) is a disease in which renal function declines sharply and is the most common complication of critical patients (1). Poor prognosis and high mortality rate are associated with AKI (2), and it is also an important contributing factor to the global increase in the incidence of chronic kidney disease (1). Ischemia-reperfusion injury (IRI) is a leading clinical cause of AKI (3), which is characterized by initial restriction of blood supply to the organs, and then restoration of perfusion followed by reoxidation, thereby aggravating tissue damage (4). The pathogenesis of IRI, which is a process involving oxidative stress, inflammation, calcium overload, and apoptosis, is complex (5). Unfortunately, there is currently no effective treatment to prevent AKI induced by IRI or promote recovery from AKI (6). Therefore, how to effectively prevent renal IRI and reduce the mortality of AKI patients has become an important clinical problem that needs to be urgently addressed.

Increasingly, evidence has indicated that T cells, dendritic cells, neutrophils, and macrophages in both innate and adaptive immunity play regulatory roles in the pathogenesis of AKI (7,8). Among them, macrophages play key roles in renal injury, inflammation, and fibrosis (9). Generally, macrophages display 2 types of activation phenotypes, including M1-macrophages and M2-macrophages polarization (10). The M1-macrophages highly express pro-inflammatory cytokines, including interleukin (IL)-23, 12, 6, 1, inducible nitric oxide synthase (iNOS), and tumor necrosis factor-α (TNF-α), which aggravate kidney tissue damage (11,12). The M2-macrophages highly express transforming growth factor-β (TGF-β), arginase-1, and IL-10, which exert anti-inflammatory effects of promoting inflammation subsidence and wound healing (12). Modulating the phenotypic transition of macrophages from M1 to M2 is a complex and variable process. Chen *et al.* found that regulation of macrophage polarization by nuclear receptor PPARγ, nuclear receptors PPARγ can promote the polarization of macrophages to the M2 phenotype (13). However, during AKI, M2-macrophages cannot completely prevent M1-macrophages from aggravating kidney tissue damage and causing chronic kidney disease (9). Therefore, slowing down the pro-inflammatory effect of M1-macrophages in kidney injury may be more conducive to the recovery of AKI.

V-set and immunoglobulin domain containing protein 4 (VSIG4) is a newly discovered costimulatory molecule of the B7 family specifically expressed in macrophages, also known as complement receptor of the immunoglobulin Ig superfamily molecule (CRIg) (14,15). The report has found that VSIG4 deletion significantly increases the secretory activity of macrophages, which is mainly reflected in the regulation of IL-1β, IL-6, and TNF-α secretion, to exacerbate hepatic inflammation and fibrosis induced by high fat diet (16). Up to now, no direct relationship between VSIG4 expression of macrophage and the development of acute renal injury has been reported. In our study, we explored the role of VSIG4 overexpression in M1-macrophage activation of the mouse macrophage cell line, RAW267.4, induced by lipopolysaccharide (LPS). Moreover, the effect of VSIG4 overexpression in RAW267.4 on HK-2 cells, as well as the result of VSIG4 knockout on the kidney pathological changes in IRI mice were further examined to achieve the purpose of seeking new ideas for the treatment of renal interstitial inflammation. We present the following article in accordance with the ARRIVE reporting checklist (available at https://atm.amegroups.com/article/view/10.21037/atm-22-1621/rc).

Methods

Cell incubation

We purchased RAW264.7 and HK-2 cells from the Shanghai Cell Bank of Chinese Academy of Sciences (Shanghai, China). The RAW264.7 and HK-2 cells were incubated in Dulbecco's modified Eagle medium (DMEM; Gibco, Carlsbad, CA, USA) containing 10% fetal bovine serum (FBS), 100 U/mL streptomycin, and 100 U/mL penicillin at 37 ℃ in a humid incubator with 5% CO_2.

Plasmid transfection

The *VSIG4* gene was cloned into pcDNA3 plasmids to obtain plasmids of VSIG4 overexpression (over-VSIG4). Empty pcDNA3 plasmids were used as the negative control (NC). The RAW264.7 cells were transfected with overexpressed VSIG4 via Lipofectamine® 2000 (Invitrogen, Carlsbad, CA, USA) based on the manufacturer's protocol. We then used 1 μg of plasmids to transfect $1×10^5$ RAW264.7. 48 hours after transfection. The protein and messenger RNA (mRNA) levels of VSIG4 were determined using western blot and quantitative real-time polymerase chain reaction (qPCR). Subsequent experiments were performed using the above-mentioned transfected cells.

M1-macrophage activation of RAW264.7

The RAW264.7 cells transfected with over-VSIG4 or pcDNA3 were induced by 2 µg/mL LPS (Invitrogen, USA) or no-LPS. The processed cells were grouped into Control, LPS, LPS + pcDNA3, and LPS + over-VSIG4 groups. Then, the morphology of RAW264.7 cells were observed under a light microscope (Nikon Eclipse TI-SR, Japan). The M1-macrophage surface markers iNOS and cluster of differentiation 86 (CD86) were tested by flow cytometry. After that, 3-(4,5-dimethylthiazol-2-yl)-2,5-diphenyl tetrazolium bromide (MTT) and 5-ethynyl-2'-deoxyuridine (EdU) staining were used to analyze the cell proliferation ability, and the IL-6, TNF-α, and IL-1β levels within RAW264.7 cells and supernatant of RAW264.7 were measured via qPCR and enzyme linked immunosorbent assay (ELISA), respectively.

Co-culture of HK-2 cells and RAW264.7

The RAW264.7 cells or RAW264.7 cells transfected with over-VSIG4 were co-incubated with LPS-induced HK-2 cells in a Transwell system. Then, 1 mL of HK-2 cells (1×10^4 cells) induced by 2 µg/mL LPS or no-LPS were plated on the bottom plate of the chamber. After 4 hours, 1 mL of RAW264.7 or RAW264.7 transfected with over-VSIG4 (1×10^4 cells) were plated on the upper chamber. Co-cultured cells were also divided into 4 groups, including HK-2, HK-2 + LPS, HK-2 + LPS + RAW264.7, and HK-2 + LPS + (RAW264.7 + over-VSIG4) groups. Then, the morphology of HK-2 cells was compared under a light microscope. We used EdU to detect the proliferation ability of HK-2 cells. Flow cytometry and western blot were used for detecting HK-2 cell apoptosis level.

Flow cytometric analysis

To analyze the surface markers of M1-macrophages, 5×10^5 cells were cultured with anti-CD86 and anti-iNOS monoclonal antibodies on ice. After 15 minutes, fluorescein isothiocyanate (FITC)-conjugated antibodies were added and incubated for 40 minutes on ice. Cells were washed once in phosphate-buffered saline (PBS) and detected via a FACSCalibur instrument [Becton, Dickinson, and Co. (BD) Biosciences; San Jose, CA, USA]. The BD FACSuite™ version 1.01 (BD, USA) was used for signal acquisition and result analysis.

MTT assay

The RAW264.7 cells in the in Control, LPS, LPS + pcDNA3, and LPS + over-VSIG4 groups were seeded in 96 well plates (5×10^4 cells/well). Then, RAW264.7 cells were treated with LPS for 24, 48, and 72 hours at 37 ℃, respectively. We added 10 µL 5 mg/mL MTT solution into 96 well plates at 37 ℃. After 4 hours, the supernatant was removed and dimethyl sulfoxide (DMSO) was added. Then, the absorbance was observed using a Multi Well Micro Plate Reader (Bio Rad; Hercules, CA, USA) at 560 nm. Cell viability was analyzed.

EdUproliferation ability analysis

We used EdU to detect cell proliferation. Briefly, RAW264.7 and HK-2 cells were stained with 10 µM EdU (RiboBio, Guangzhou, China) at 37 ℃ for 2 hours. Then, the cells were fixed with 4% polyoxymethylene at 25 ℃ for 30 minutes, decolorized with 2 mg/mL glycine at 25 ℃ for 5 minutes, and stained with Hoechst 33342 at 25 ℃ for 30 minutes. The fluorescent signals of RAW264.7 and HK-2 cells were analyzed using an inverted fluorescence microscope. Finally, the semi-quantitative analysis of EdU ratio was as follows: number of EdU positive cells/number of Hoechst 33342 positive cells ×100%.

ELISA

The levels of inflammatory factors in the supernatant of RAW264.7 were detected using the following reagent kits: TNF-α Mouse ELISA Kit (RayBiotech, Norcross, GA, USA), IL-6 Mouse ELISA Kit (Thermo Fisher Scientific, Waltham, MA, USA), and IL-1β Mouse ELISA Kit (Thermo Fisher Scientific, USA), based on the manufacturer's protocols.

qPCR

Total RNA in RAW264.7 cells was extracted via TRIzol reagent (Invitrogen, Waltham, MA, USA) based on the manufacturer's protocol. Complementary DNA (cDNA) was synthesized by QuantiTect Reverse Transcription Kit (Qiagen, Duesseldorf, Germany) with the reverse transcription (RT) thermal conditions as follows: 42 ℃ for 15 minutes and 95 ℃ for 3 minutes. Then, the qPCR reaction was carried out in 50 µL volumes via SYBR Green

Page 4 of 14

Li et al. VSIG4 overexpression inhibits M1-macrophages activation

Table 1 The primer sequences for qPCR

ID	Sequence (5'-3')	Product length (bp)
β-actin F	CATTGCTGACAGGATGCAGA	139
β-actin R	CTGCTGGAAGGTGGACAGTGA	
IL6 F	CTGCAAGAGACTTCCATCCAG	131
IL6 R	AGTGGTATAGACAGGTCTGTTGG	
TNF-α F	CCCACGTCGTAGCAAACC	212
TNF-α R	GATAGCAAATCGGCTGACGG	
IL-1β F	TGATAACCTGCTGGTGTGTG	200
IL-1β R	AGGCCACAGGTATTTTGTCG	
VSIG4 F	CCTGGGCCACCTAATAGTGC	118
VSIG4 R	GCCTCTCAGGGGATCATAGAT	

qPCR, quantitative polymerase chain reaction; TNF-α, tumor necrosis factor-α; IL-6, interleukin 6; IL-1β, interleukin 1β.

PCR master mix (Solarbio, Beijing, China) in an ABI 7900HT thermocycler (Thermo Fisher Scientific, USA). The qPCR thermocycling conditions were as follows: 95 ℃ for 15 minutes, 95 ℃ for 30 seconds (40 cycles), 60 ℃ for 30 seconds, and 72 ℃ for 2 minutes. All primers are listed in *Table 1*. The $2^{-\Delta\Delta Ct}$ was executed to quantify the mRNA levels. Glyceraldehyde 3-phosphate dehydrogenase (GAPDH) was used as the internal control.

Western blot

Cells were lysed using radioimmunoprecipitation assay (RIPA) lysis buffer. A bicinchoninic acid (BCA) assay kit (Beyotime, Shanghai, China) was used to detect the protein concentration. We then separated 20 µg of lysate proteins by 10% sodium dodecyl sulfate polyacrylamide gel electrophoresis (SDS-PAGE) and transferred to a polyvinylidene fluoride (PVDF) membrane. The membranes were blocked using 0.05% tris-buffered saline with Tween 20 (TBST) including 5% non-fat milk at room temperature for 2 hours and incubated with anti-VSIG4, B-cell lymphoma-2 (Bcl-2), Bcl-2 associated X (Bax), Cleaved-caspase-9, Cleaved-caspase-3, and GAPDH antibodies at 4 ℃ overnight. The cells were then washed with TBST and the membranes were incubated with secondary antibodies conjugated to horseradish peroxidase at room temperature for 2 hours. Bands were detected using the hypersensitive electrochemiluminescence (ECL) kit

(Beyotime, China). The gray value of protein imprinting was analyzed using ImageJ (National Institutes of Health, Bethesda, MD, USA).

Cell apoptosis analysis

The apoptotic level of HK-2 cells was detected with Annexin V-FITC Apoptosis Detection Kit (BD Pharmingen, San Diego, CA, USA). The HK-2 cells were suspended at 5×10^5/mL in Annexin binding buffer of Annexin V FITC and incubated with 10 µL Annexin V-FITC for 15 minutes. Then, the suspension was incubated with 5 µL propidium iodide (PI) for 15 minutes at room temperature. Samples were analyzed by a FACSCalibur instrument (BD Biosciences, USA) with a 488 nm excitation and 530 nm emission for FITC and a 575 nm excitation and 610 nm emission for PI. The data were quantified by the BD FACSuite™ version 1.01.

Construction of kidney IRI model

We purchased 10 male wild and 10 male VSIG4 knockout C57BL/6 mice (6 weeks old and weighing 20–25 g) from the Experimental Animal Center at in the Third Military Medical University (Chongqing, China). All animal practices were conducted according to the National Institutes of Health Guidelines on the Use of Laboratory Animals and authorized by the Army Medical University (Third Military Medical University) Ethics Committee (No. AMUWEC20184502) (17). The state of AKI was induced in C57BL/6 mice through an ischemia followed by reperfusion method (18,19). Briefly, during model construction, mice were aseptically prepared and placed on a constant temperature table to maintain a body temperature of 37 ℃. Simultaneously, buprenorphine hydrochloride (0.01 mg/kg) was used to anesthetize the mice. A midline abdominal incision was made, and 2 renal pedicles were clipped with a non-invasive microaneurysm clamp for 19 minutes. Then, the incision was closed, followed by the intraperitoneal injection of 0.9% warmed saline. After 0–72 hours of recovery, mice were euthanized and the kidneys were harvested for pathological analysis.

Hematoxylin and eosin staining

The specimens were dehydrated in a graded ethanol series and embedded in paraffin. Then, 5 µm thick sections were deparaffinized in xylene and rehydrated in graded ethanol and water. Sections were stained with hematoxylin for

5 minutes and eosin for 2 minutes, washed with water, dehydrated with gradient alcohol, treated with xylene twice for 5 minutes each time, and sealed with neutral resin. The prepared sections were observed under an optical microscope.

Immunohistochemistry (IHC)

Sections were deparaffinized in xylene, rehydrated in graded ethanol and water. Antigen retrieval was carried out based on 0.1 M sodium citrate, and endogenous peroxidase activity was inhibited by 0.3% H_2O_2 for 10 minutes. The sections were washed several times with PBS and pre-incubated with 5% bovine serum albumin (BSA) for 20 minutes. The sections were cultured with mouse anti-iNOS antibody at 4 ℃ overnight and the secondary goat anti-mouse antibody labeled with horseradish peroxidase at 37 ℃ for 30 minutes. The color reaction was developed with 3,3'-diaminodenzidine (DAB) and counterstained with hematoxylin. The prepared sections were observed under an optical microscope.

Statistics

All experiments were repeated 3 times. Data were analyzed with the software GraphPad Prism 8.0.2 (GraphPad Software, Inc., La Jolla, CA, USA), using one-way analysis of variation (ANOVA), followed by the Tukey's multiple comparisons test for multiple comparisons. A P value <0.05 was considered statistically significant.

Results

VSIG4 overexpression inhibited the morphology and the activation of M1-macrophages

We first constructed plasmids of VSIG4 overexpression (over-VSIG4), and transfected the over-VSIG4 into RAW264.7 to analyze the role of VSIG4 on the surface markers of M1-macrophages in LPS-stimulated RAW264.7. The qPCR analysis indicated that mRNA expression of VSIG4 in RAW264.7 transfected with over-VSIG4 was greatly higher than that of the control group (*Figure 1A*). Simultaneously, the western blot and semi-quantitative analysis revealed that the protein of VSIG4 in RAW264.7 transfected with over-VSIG4 was prominently higher that of the control group (*Figure 1B*), indicating that the

over-VSIG4 had been successfully transfected into the RAW264.7. The morphology of RAW264.7 under different treatment conditions was further observed. The results revealed that the RAW264.7 cells had an irregular round shape in Control group, and then LPS treatment induced changes in the fibrous morphology of M1-macrophages (*Figure 1C*). Contrarily, VSIG4 overexpression relieved the changes in the fibrous morphology of macrophages induced by LPS (*Figure 1C*). In addition, the levels of CD86 and iNOS in RAW264.7 induced through LPS were upregulated compared to the Control group; however, VSIG4 overexpression suppressed expression of CD86 and iNOS in RAW264.7 induced with LPS. We could conclude that LPS stimulated M1-polarization in RAW264.7 cells, and VSIG4 overexpression could alleviate this phenomenon (*Figure 1D*).

VSIG4 overexpression inhibited the inflammatory factor expression of M1 macrophages in RAW264.7 stimulated with LPS

Furthermore, the EdU staining and MTT assays revealed that LPS treatment reduced the viability of RAW264.7 cells (*Figure 2A-2C*). The viability of RAW264.7 cells overexpressing VSIG4 treated with LPS were significantly upregulated compared to RAW264.7 treated with LPS, indicating that LPS decreased the viability of RAW264.7 and VSIG4 overexpression could relieve this phenomenon (*Figure 2A-2C*). The presence of macrophage M1 polarization indicated the high expression of pro-inflammatory factors. In order to show the regulatory effect of VSIG4 on macrophage polarization, we used qPCR and ELISA to detect the levels of inflammatory factors in RAW264.7 induced by LPS (*Figure 2D-2I*). The qPCR results revealed that mRNA expression of inflammatory factors was greatly increased in RAW264.7 cells stimulated with LPS compared to the Control group (*Figure 2D-2F*). The mRNA levels of inflammatory factors were greatly decreased in RAW264.7 cells stimulated with LPS and transfected with over-VSIG4 compared to the LPS group (*Figure 2D-2F*). Simultaneously, the RAW264.7 cell supernatant tested by the ELISA experiment showed the same result, as did that of with qPCR assay (*Figure 2G-2I*). These results further illustrated that LPS stimulated M1 polarization in RAW264.7, while VSIG4 could inhibit M1 activation in RAW264.7 cells.

Page 6 of 14

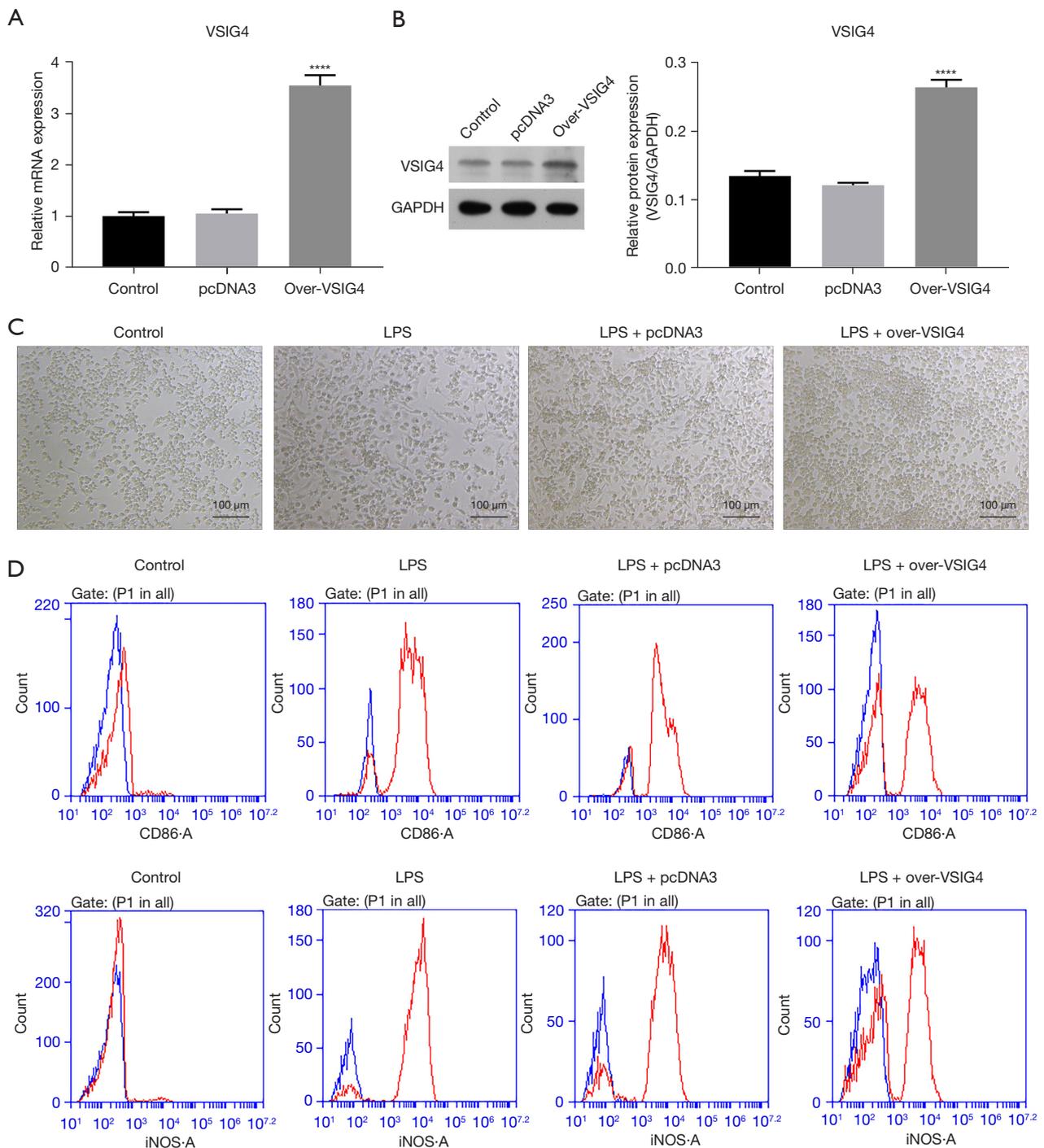Li et al. VSIG4 overexpression inhibits M1-macrophages activation

Figure 1 The effect of VSIG4 overexpression on the morphology and markers of RAW264.7 induced by LPS. (A) The mRNA expression of VSIG4 in RAW264.7 transfected with overexpression plasmids of VSIG4 (over-VSIG4) was detected by qPCR. (B) The protein expression and semi-quantitative analysis of VSIG4 in RAW264.7 cells transfected with over-VSIG4 was analyzed by western blot. (C) The morphology changes of RAW264.7 transfected with over-VSIG4 were observed in light microscope. (D) The expression level of surface markers-CD86 and iNOS of RAW264.7 transfected with over-VSIG4 through flow cytometer. ****, P<0.0001 represents significance. VSIG4, V-set and immunoglobulin domain containing 4; GAPDH, glyceraldehyde 3-phosphate dehydrogenase; LPS, lipopolysaccharide; qPCR, quantitative polymerase chain reaction; CD86, cluster of differentiation 86; iNOS, inducible nitric oxide synthase.
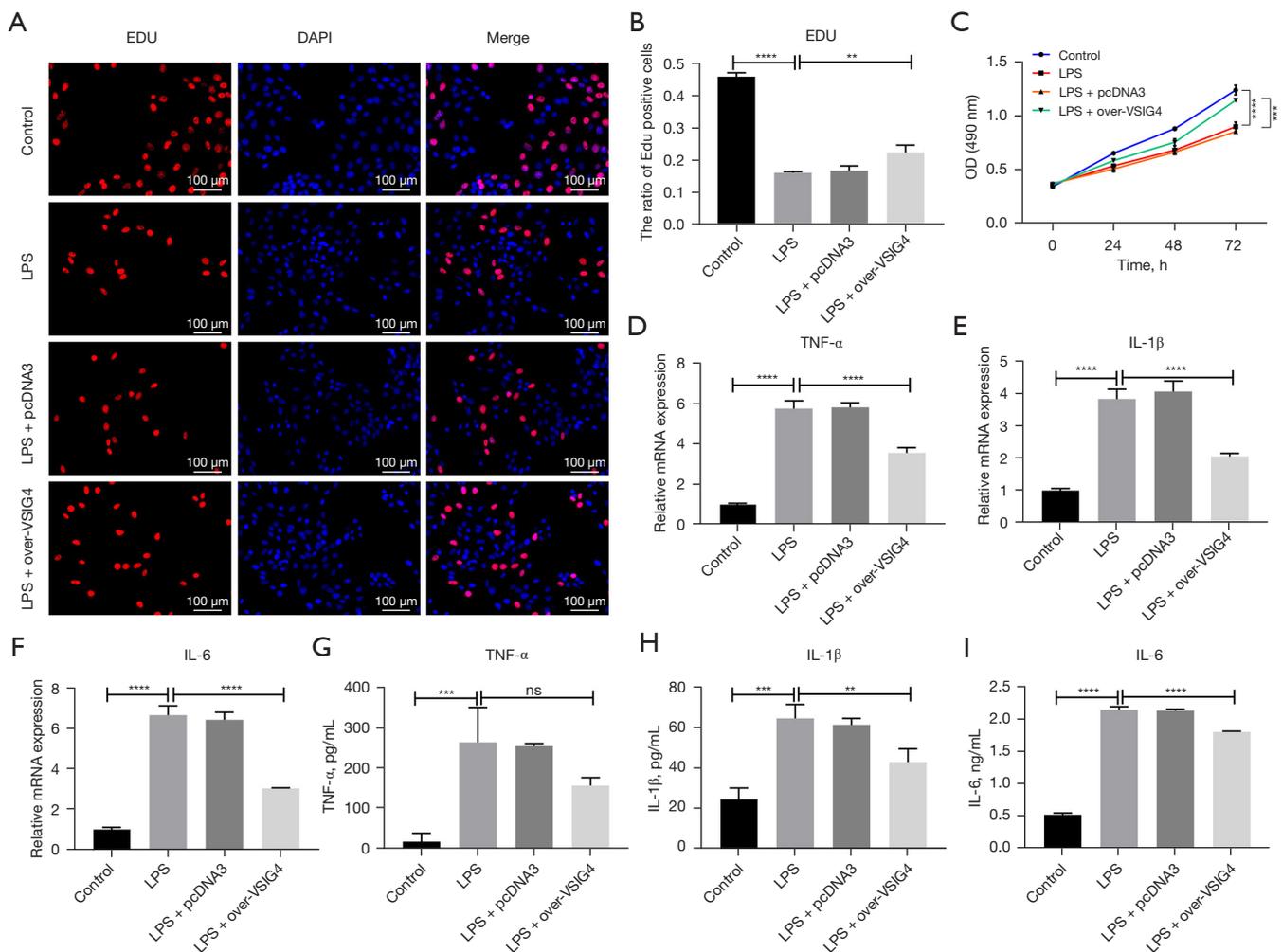
Figure 2 The effect of VSIG4 overexpression on the proliferation and inflammatory factors of RAW264.7 induced by LPS. (A) The proliferation capacity of RAW264.7 transfected with plasmids of VSIG4 overexpression (over-VSIG4) was detected by EdU staining. (B) The semi-quantitative analysis of EdU positive cells ratio in graph A. (C) The viability of RAW264.7 transfected with over-VSIG4 was analyzed by MTT assay. (D-F) The inflammatory factor levels in RAW264.7 transfected with over-VSIG4 were analyzed by qPCR assay. (G-I) The inflammatory factor protein levels in the supernatant of RAW264.7 transfected with over-VSIG4 were analyzed by ELISA assay. **, $P<0.01$, ***, $P<0.001$, and ****, $P<0.0001$ represent significance; ns, no significance. VSIG4, V-set and immunoglobulin domain containing 4; LPS, lipopolysaccharide; MTT, 3-(4,5-dimethylthiazol-2-yl)-2,5-diphenyl tetrazolium bromide; EdU, 5-ethynyl-2'-deoxyuridine; qPCR, quantitative polymerase chain reaction; ELISA, enzyme-linked immunosorbent assay.

The RAW264.7 cells overexpressing VSIG4 promoted the proliferation of HK-2 cells stimulated with LPS

In order to further simulate the effect of M1-macrophages polarization on AKI *in vivo*, HK-2 cells stimulated with LPS were co-cultured with RAW264.7 cells overexpressing VSIG4 to explore the effect of RAW264.7 overexpressing VSIG4 on HK-2 cells. The results revealed that HK-2 cells were round adherent cells, and the cells merged into a cobblestone shape in the control group (*Figure 3A*). After HK-2 cells were treated with LPS, they changed from a round shape to an elongated spindle shape, and the connection between the cells became loose (*Figure 3A*). In addition, when HK-2 cells induced with LPS were co-cultured with RAW264.7, cell connections were looser, indicating that RAW264.7 enhanced abnormality of HK-2 cells (*Figure 3A*). However, when HK-2 cells induced with
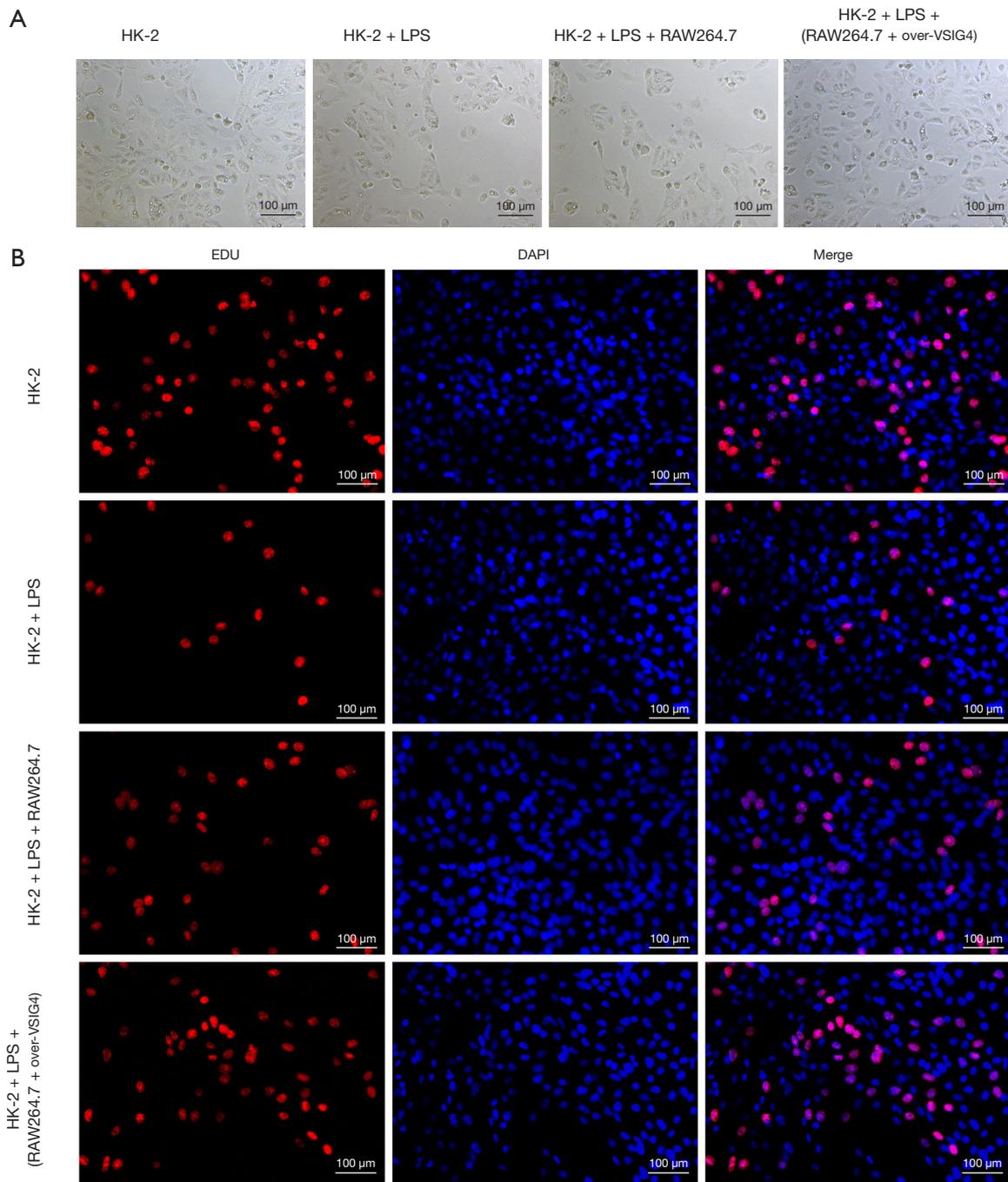
Figure 3 The effect of VSIG4 overexpression in RAW264.7 on the morphology and multiplication of HK-2 cells induced by LPS. (A) The morphology changes of HK-2 cells, which were co-cultured with RAW264.7 overexpressing VSIG4, induced by LPS were observed in light microscope. (B) The proliferation capacity of HK-2 cells, which were co-incubated with RAW264.7 overexpressing VSIG4, induced by LPS was detected by EdU staining. VSIG4, V-set and immunoglobulin domain containing 4; LPS, lipopolysaccharide; EdU, 5-ethynyl-2'-deoxyuridine.

LPS were co-cultured with RAW264.7 overexpressing VISG4, their morphology was partially restored to normal, indicating that VISG4 could decrease the abnormality of HK-2 cells stimulated with LPS and RAW264.7 (*Figure 3A*). In addition, the proliferation ability of the HK-2 cells was further tested by EdU staining (*Figure 3B*). The results showed that LPS reduced HK-2 cells proliferation and RAW264.7 exacerbated the low proliferation of HK-2 cells stimulated with LPS, indicating that M1 macrophages might accelerate the low proliferation level of HK-2 cells stimulated with LPS (*Figure 3B*). Moreover, when the 2 kinds of cells were co-cultured, the proliferation ability of HK-2 cells was improved after RAW264.7 cells were transfected with the over-VSIG4, indicating that VSIG4 might promote the proliferation of HK-2 cells by inhibiting the polarization of M1-macrophages (*Figure 3B*).

VSIG4 overexpression in RAW264.7 inhibited the apoptotic level of HK-2 cells stimulated with LPS

After exploring the effect of RAW264.7 cells overexpressing VSIG4 on the proliferation ability of HK-2 cells, we further studied its role in the apoptosis of HK-2 cells. After LPS treatment, the early and late apoptotic percentage of HK-2 cells was 21.4%, which was higher than the 4.7% of the control group (*Figure 4A*). After co-culture with RAW264.7, the early and late apoptotic percentage of HK-2 cells was 25% (*Figure 4A*), suggesting that LPS induced the apoptosis of HK-2 cells, while RAW24.7 accelerated LPS-induced apoptosis of HK-2 cells. However, after transfection with over-VSIG4, the apoptosis level of HK-2 cells was 12.7%, which was lower than that of HK-2 cells stimulated with LPS (*Figure 4A*), indicating that VSIG4 overexpression in RAW264.7 cells inhibited the apoptotic level of HK-2 cells stimulated with LPS. Furthermore, the level of apoptotic protein was tested. The western blot analysis demonstrated that LPS significantly upregulated the Bax and Cleaved-caspase-3 protein expression and downregulated Bcl-2 and Cleaved-caspase-9 protein (*Figure 4B*). However, after co-culture with RAW264.7, the above-mentioned protein expression was further enhanced (*Figure 4B*). When RAW264.7 cells overexpressed VSIG4, the above-mentioned protein expression was reversed (*Figure 4B*). These results further indicated that M1 polarization of RAW264.7 could accelerate the apoptosis of HK-2 cells, and overexpression of VSIG4 could alleviate the apoptosis of HK-2 cells by inhibiting M1 macrophages activation.

VSIG4 knockout aggravated AKI induced by IRI

After testing the effect of VSIG4 on M1 type polarization of macrophages and HK-2 cells injury at the cell level *in vitro*, we further tested the effect of VSIG4 on the diseased kidney tissue of AKI mice at the animal level *in vivo*. We established wild type (WT) and VSIG4 knockout (KO-VSIG4) mice with IRI and detected the pathological changes of kidney tissue of mice. The hematoxylin and eosin (H&E) staining analysis showed that morphology and structure of the kidney tissue of the WT mice were normal in the NC group (*Figure 5A*). There was no edema or necrosis of epithelial cells, mesenchymal edema, and infiltration of inflammatory cells in the NC group (*Figure 5A*). Simultaneously, the renal tubules were arranged neatly in the NC group. In addition, the morphology and structure of the kidney tissue of the WT mice were obviously abnormal in IRI group (*Figure 5A*). The epithelial cells showed obvious swelling and necrosis in IRI group (*Figure 5A*). Damaged kidney tissue also showed infiltration of inflammatory cells and interstitial edema phenomenon in IRI group (*Figure 5A*). However, the kidney damage in VSIG4 knockout mice was significantly worse, suggesting that VSIG4 knockout might increase AKI in mice indued by IRI. Furthermore, the results of IHC staining revealed that the level of iNOS in the kidney tissue of mice induced by IRI was higher compared to the NC group, implying the infiltration and activation of an abundance of M1-macrophages in IRI mice (*Figure 5B*). However, after VSIG4 knockout, the level of iNOS in the kidney tissue of IRI mice was increased, showing that VSIG4 knockout intensified the polarization and infiltration of M1-macrophages in AKI tissue (*Figure 5B*). It could be inferred that the knockout of VSIG4 exacerbated the AKI in IRI mice via the activation of M1-macrophages.

Discussion

Renal IRI is the main cause of AKI (20), which often occurs in kidney transplantation, nephron-sparing surgery, renal vascular surgery, and cardiac surgery (21). Many factors mediate IRI, containing the formation of reactive oxygen species and the infiltration and activation of inflammatory cells (22). Inflammation can damage renal tubules, leading to kidney tissue damage and reduced renal function (23). Among them, M1-macrophages are the critical inflammatory cells in the occurrence of AKI inflammatory damage (7,8). In this study, we discovered that VSIG4 overexpression inhibited the activation of M1-macrophages and explored
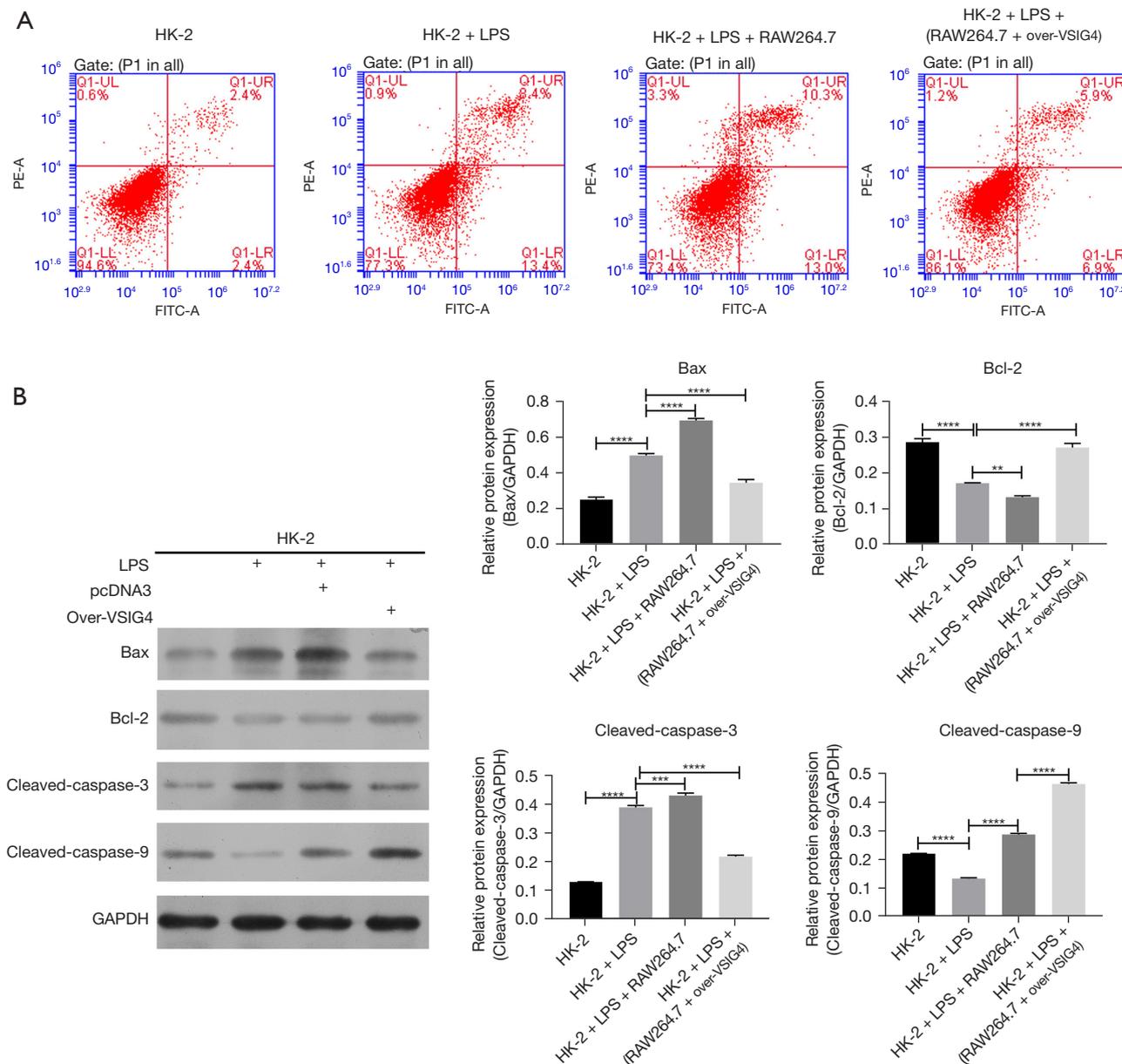
Page 10 of 14

Li et al. VSIG4 overexpression inhibits M1-macrophages activation

Figure 4 The effect of VSIG4 overexpression in RAW264.7 on the apoptotic level of HK-2 cells induced by LPS. (A) The apoptotic ratio of HK-2 cells, which were co-cultured with RAW264.7 overexpressing VSIG4, induced by LPS were detected via flow cytometer. (B) The Cleaved-caspase-9, Cleaved-caspase-3, Bax, and Bcl-2 protein levels in HK-2 cells, which were co-incubated with RAW264.7 overexpressing VSIG4, induced by LPS were analyzed by EdU staining. Semi-quantitative analysis of the protein was carried out through ImageJ software. **, $P<0.01$, ***, $P<0.001$, and ****, $P<0.0001$ represent significance. +, what is treated to the cell. VSIG4, V-set and immunoglobulin domain containing 4; LPS, lipopolysaccharide; GAPDH, glyceraldehyde 3-phosphate dehydrogenase; EdU, 5-ethynyl-2'-deoxyuridine.

the effect of macrophages overexpressing VSIG4 on HK-2 cells. Our results indicated that RAW264.7 overexpressing VSIG4 could alleviate low proliferation and high apoptotic percentage in HK-2 cells stimulated with LPS.

Simultaneously, *in vivo* animal experiments indicated that the kidney tissue of AKI mice showed obvious lesions and iNOS expression after VSIG4 knockout, indicating that VSIG4 knockout promoted the infiltration of M1-
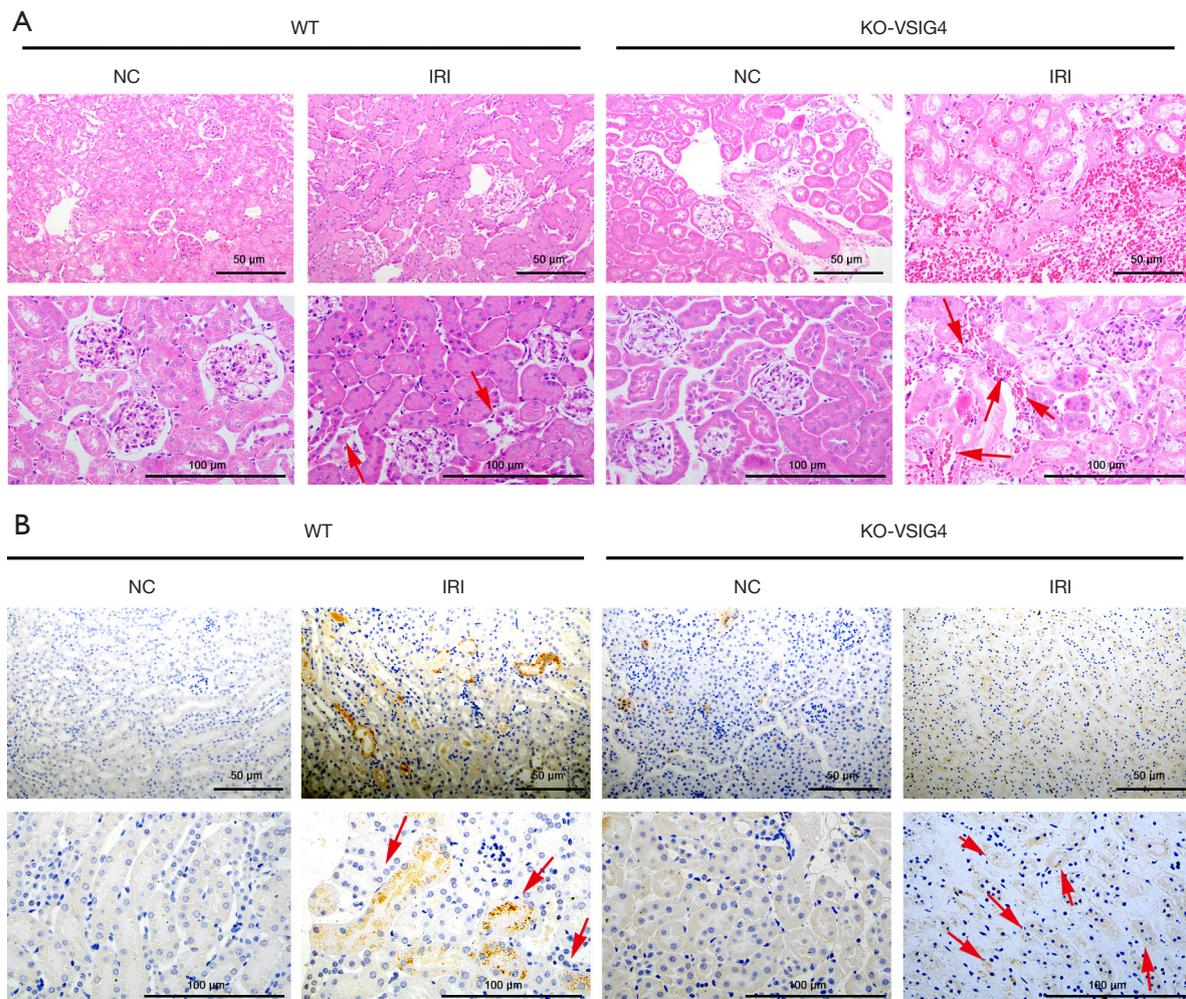
Figure 5 The effect of VSIG4 knockout on pathological changes of renal tissue in mice with IRI. (A) The pathological changes of renal tissue in VSIG4 knockout mice with IRI was analyzed by H&E staining (red arrows, inflammatory cells). (B) The iNOS expression of renal tissue in VSIG4 knockout mice with IRI was detected by IHC staining (red arrows, positive). VSIG4, V-set and immunoglobulin domain containing 4; WT, wild type; KO-VSIG4, knock out VSIG4 gene; NC, negative control; IRI, ischemia reperfusion injury; H&E, hematoxylin and eosin; iNOS, inducible nitric oxide synthase; IHC, immunohistochemistry.

macrophages in the damaged kidney tissue and accelerated kidney tissue lesions. The above results explained that *VSIG4* might be a therapeutic gene for AKI induced IRI.

Generally, classically activated M1-macrophages secrete abundant chemokines, including IL-1β, IL-6, and TNF-α, and cytokines, which kill microorganisms and promote inflammation (24,25). However, excessive activation of M1-macrophages causes inflammatory pathological damage, leading to a variety of inflammatory diseases, including diabetes (26), rheumatoid arthritis (27), and AKI (28). Research has shown that hydroxyapatite increases the expression level of reactive oxygen species, C-C motif

chemokine ligand 2, and TNF-α in HK-2 cells, and also enhances the apoptotic protein ratio of Bax/Bcl-2 (29). When M1-macrophages are added to HK-2 cells for co-culture, the injury and apoptosis of HK-2 cells are aggravated (29). Although macrophage depletion can relieve renal injury in the early stage, it also impairs the ability to recover in the late stage (30), suggesting that direct macrophage loss is not a good treatment for AKI recovery. In our research, we found that VSIG4 overexpression suppressed the activation of M1-macrophages in RAW264.7 cells induced by LPS, and that RAW264.7 cells overexpressing VSIG4 could also alleviate low

Page 12 of 14

Li et al. VSIG4 overexpression inhibits M1-macrophages activation

proliferation and high pro-apoptotic proteins level in HK-2 cells stimulated with LPS. Therefore, it could be inferred that adjusting the polarization direction of macrophages contributes to the tubular epithelial cell proliferation and recovery of AKI.

In addition, Lyu *et al.* have long shown that VSIG4 overexpression can inhibit the microglial M1-macrophage polarization in middle cerebral artery occlusion mice by downregulating the expression of CD16, CD11b, iNOS, and IL-6, and exert an anti-inflammatory effect through blocking toll-like receptor 4/nuclear factor kappa B signaling (14). Overexpression of VSIG4 improves murine hepatitis virus strain-3-stimulated fulminant hepatitis by enhancing M1-macrophages activation via reprogramming mitochondrial pyruvate metabolism (31). It can be inferred that *VSIG4* is an important gene that inhibits the activation of M1 pro-inflammatory macrophages. Moreover, CD3/4/8 and interferon-γ (IFN-γ) levels are extremely lower in unilateral ureteral obstruction (UUO)-induced VSIG$^{+/+}$ mice than those in the (UUO)-induced VSIG$^{-/-}$ mice, indicating that macrophage-expressed VSIG-4 relieves renal tubulointerstitial injury by inhibiting T cell infiltration and the expression of inflammatory factors (32). Inflammation, as a major driver of recruitment of immune cells (including macrophages), is closely associated with the development of the disease. Nuclear transcription factor kappa B (NF-κB), as one of the major inflammatory regulators, is the key transcription factor that promotes the gene transcription of inflammatory cytokines. It has been reported that the inhibition of activation of M1 macrophages by inhibiting the expression of NF-κB signal pathway negative regulator socs-1. Therefore, it plays an important role in regulating the activation of M1 macrophages and the inflammation of Tubulointerstitium by NF-κB/socs-1 signaling pathway (33). This suggests that VSIG4 overexpression may regulate the polarization of M1 macrophages through the NF-κB signaling pathway, which may play a role in regulating acute renal injury. Furthermore, we found that after VSIG4 knockout, the kidney tissue of AKI mice showed obvious lesions and iNOS expression, indicating that VSIG4 knockout promoted the infiltration of M1-macrophages in the damaged kidney tissue and accelerated kidney tissue lesions in our research. Overall, VSIG4 not only inhibits T cell infiltration, but also inhibits the activity of pro-inflammatory M1-macrophages to relieve AKI; however, its underlying mechanism still needs to be further explored.

Conclusions

Overexpression of VSIG4 alleviates the lesions of kidney tissue in AKI mice via inhibiting the secretion of inflammatory factors in M1-macrophage. The *VSIG4* gene might be a potential therapeutic target to AKI induced by IRI, providing a novel idea for the treatment of renal interstitial inflammation and fibrosis.

Acknowledgments

Footnote

Reporting Checklist: The authors have completed the ARRIVE reporting checklist. Available at https://atm.amegroups.com/article/view/10.21037/atm-22-1621/rc

Data Sharing Statement: Available at https://atm.amegroups.com/article/view/10.21037/atm-22-1621/dss

Conflicts of Interest: All authors have completed the ICMJE uniform disclosure form (available at https://atm.amegroups.com/article/view/10.21037/atm-22-1621/coif). The authors have no conflicts of interest to declare.

Ethical Statement: The authors are accountable for all aspects of the work in ensuring that questions related to the accuracy or integrity of any part of the work are appropriately investigated and resolved. All animal practices were conducted according to the National Institutes of Health Guidelines on the Use of Laboratory Animals and authorized by the Army Medical University (Third Military Medical University) Ethics Committee (No. AMUWEC20184502).

Open Access Statement: This is an Open Access article distributed in accordance with the Creative Commons Attribution-NonCommercial-NoDerivs 4.0 International License (CC BY-NC-ND 4.0), which permits the non-commercial replication and distribution of the article with the strict proviso that no changes or edits are made and the original work is properly cited (including links to both the formal publication through the relevant DOI and the license). See: https://creativecommons.org/licenses/by-nc-nd/4.0/.

References

1. Liu SS, Chen YY, Wang SX, et al. Protective effect of dabrafenib on renal ischemia-reperfusion injury in vivo and in vitro. Biochem Biophys Res Commun 2020;522:395-401.

2. Hosszu A, Fekete A, Szabo AJ. Sex differences in renal ischemia-reperfusion injury. Am J Physiol Renal Physiol 2020;319:F149-54.

3. Jansen MPB, Huisman A, Claessen N, et al. Experimental thrombocytopenia does not affect acute kidney injury 24 hours after renal ischemia reperfusion in mice. Platelets 2020;31:383-91.

4. Yan HF, Tuo QZ, Yin QZ, et al. The pathological role of ferroptosis in ischemia/reperfusion-related injury. Zool Res 2020;41:220-30.

5. Nieuwenhuijs-Moeke GJ, Pischke SE, Berger SP, et al. Ischemia and Reperfusion Injury in Kidney Transplantation: Relevant Mechanisms in Injury and Repair. J Clin Med 2020;9:253.

6. Tan RZ, Liu J, Zhang YY, et al. Curcumin relieved cisplatin-induced kidney inflammation through inhibiting Mincle-maintained M1 macrophage phenotype. Phytomedicine 2019;52:284-94.

7. Bonavia A, Singbartl K. A review of the role of immune cells in acute kidney injury. Pediatr Nephrol 2018;33:1629-39.

8. Jang HR, Rabb H. Immune cells in experimental acute kidney injury. Nat Rev Nephrol 2015;11:88-101.

9. Cao Q, Harris DC, Wang Y. Macrophages in kidney injury, inflammation, and fibrosis. Physiology (Bethesda) 2015;30:183-94.

10. Sellers RS, Mahmood SR, Perumal GS, et al. Phenotypic Modulation of Skeletal Muscle Fibers in LPIN1-Deficient Lipodystrophic (fld) Mice. Vet Pathol 2019;56:322-31.

11. Li Y, Zhai P, Zheng Y, et al. Csf2 Attenuated Sepsis-Induced Acute Kidney Injury by Promoting Alternative Macrophage Transition. Front Immunol 2020;11:1415.

12. Lee H, Fessler MB, Qu P, et al. Macrophage polarization in innate immune responses contributing to pathogenesis of chronic kidney disease. BMC Nephrol 2020;21:270.

13. Yunna C, Mengru H, Lei W, et al. Macrophage M1/M2 polarization. Eur J Pharmacol 2020;877:173090.

14. Lyu Q, Pang X, Zhang Z, et al. Microglial V-set and immunoglobulin domain-containing 4 protects against ischemic stroke in mice by suppressing TLR4-regulated inflammatory response. Biochem Biophys Res Commun 2020;522:560-7.

15. Jeon GH, Lee DS, Byun JM, et al. Immunoregulatory protein V-set and immunoglobulin domain-containing 4 is overexpressed in patients with endometriosis. J Obstet Gynaecol Res 2021;47:119-27.

16. Li Y, Sun JP, Wang J, et al. Expression of Vsig4 attenuates macrophage-mediated hepatic inflammation and fibrosis in high fat diet (HFD)-induced mice. Biochem Biophys Res Commun 2019;516:858-65.

17. Council N. Guide for the Care and Use of Laboratory Animals -- French Version. Publication, 1996;327:963-5. Available online: https://nap.nationalacademies.org/catalog/9852/guide-for-the-care-and-use-of-laboratory-animals-french-version

18. Pastor-Soler NM, Sutton TA, Mang HE, et al. Muc1 is protective during kidney ischemia-reperfusion injury. Am J Physiol Renal Physiol 2015;308:F1452-62.

19. Hörbelt M, Lee SY, Mang HE, et al. Acute and chronic microvascular alterations in a mouse model of ischemic acute kidney injury. Am J Physiol Renal Physiol 2007;293:F688-95.

20. Topdağı Ö, Tanyeli A, Akdemir FNE, et al. Preventive effects of fraxin on ischemia/reperfusion-induced acute kidney injury in rats. Life Sci 2020;242:117217.

21. Hara M, Torisu K, Tomita K, et al. Arginase 2 is a mediator of ischemia-reperfusion injury in the kidney through regulation of nitrosative stress. Kidney Int 2020;98:673-85.

22. Isenberg JS, Roberts DD. The role of CD47 in pathogenesis and treatment of renal ischemia reperfusion injury. Pediatr Nephrol 2019;34:2479-94.

23. Li C, Zheng Z, Xie Y, et al. Protective effect of taraxasterol on ischemia/reperfusion-induced acute kidney injury via inhibition of oxidative stress, inflammation, and apoptosis. Int Immunopharmacol 2020;89:107169.

24. Barrett TJ. Macrophages in Atherosclerosis Regression. Arterioscler Thromb Vasc Biol 2020;40:20-33.

25. Delprat V, Tellier C, Demazy C, et al. Cycling hypoxia promotes a pro-inflammatory phenotype in macrophages via JNK/p65 signaling pathway. Sci Rep 2020;10:882.

26. Zhang C, Han X, Yang L, et al. Circular RNA circPPM1F modulates M1 macrophage activation and pancreatic islet inflammation in type 1 diabetes mellitus. Theranostics 2020;10:10908-24.

27. Van Raemdonck K, Umar S, Palasiewicz K, et al. CCL21/CCR7 signaling in macrophages promotes joint inflammation and Th17-mediated osteoclast formation in rheumatoid arthritis. Cell Mol Life Sci 2020;77:1387-99.

28. Hou C, Mei Q, Song X, et al. Mono-macrophage-Derived MANF Protects Against Lipopolysaccharide-Induced

Page 14 of 14

Li et al. VSIG4 overexpression inhibits M1-macrophages activation

Acute Kidney Injury via Inhibiting Inflammation and Renal M1 Macrophages. Inflammation 2021;44:693-703.

29. Yu J, Deng Y, Tao Z, et al. The effects of HAP and macrophage cells to the expression of inflammatory factors and apoptosis in HK-2 cells of vitro co-cultured system. Urolithiasis 2018;46:429-43.

30. Xie X, Yang X, Wu J, et al. Trib1 Contributes to Recovery From Ischemia/Reperfusion-Induced Acute Kidney Injury by Regulating the Polarization of Renal Macrophages. Front Immunol 2020;11:473.

31. Li J, Diao B, Guo S, et al. VSIG4 inhibits proinflammatory macrophage activation by reprogramming mitochondrial pyruvate metabolism. Nat Commun 2017;8:1322.

32. Li Y, Wang YQ, Wang DH, et al. Costimulatory molecule VSIG4 exclusively expressed on macrophages alleviates renal tubulointerstitial injury in VSIG4 KO mice. J Nephrol 2014;27:29-36.

33. Lv LL, Feng Y, Wu M, et al. Exosomal miRNA-19b-3p of tubular epithelial cells promotes M1 macrophage activation in kidney injury. Cell Death Differ 2020;27:210-26.

Cite this article as: Li Y, Liu Y, Li F, Wang Y, Wang K, Zhao J. VSIG4 overexpression alleviates acute kidney injury of mice via inhibition of M1-macrophages activation. Ann Transl Med 2022;10(10):559. doi: 10.21037/atm-22-1621